



Numerical homogenization of two-phase flow in porous media

Wouter Zijl^a and Anna Trykozko^b

^a *Netherlands Institute of Applied Geoscience TNO, P.O. Box 80012, NL-3508 TA Utrecht, The Netherlands*

E-mail: w.zijl@nitg.tno.nl

^b *Interdisciplinary Centre for Mathematical and Computational Modelling, Warsaw University, ul. Pawińskiego 5a, 02-106 Warsaw, Poland*

E-mail: aniat@icm.edu.pl

Received 15 June 2001; accepted 13 December 2001

Homogenization has proved its effectiveness as a method of upscaling for linear problems, as they occur in single-phase porous media flow for arbitrary heterogeneous rocks. Here we extend the classical homogenization approach to nonlinear problems by considering incompressible, immiscible two-phase porous media flow. The extensions have been based on the principle of *preservation of form*, stating that the mathematical form of the fine-scale equations should be preserved *as much as possible* on the coarse scale. This principle leads to the required extensions, while making the physics underlying homogenization transparent. The method is process-independent in a way that coarse-scale results obtained for a particular reservoir can be used in any simulation, irrespective of the scenario that is simulated. Homogenization is based on steady-state flow equations with periodic boundary conditions for the capillary pressure. The resulting equations are solved numerically by two complementary finite element methods. This makes it possible to assess a posteriori error bounds.

Keywords: finite elements, homogenization, independency, mobility, process, two-phase flow

1. Introduction

There is a large and growing literature on upscaling techniques applied to porous media flow. Single-phase flow related scale-up is routinely performed nowadays and a large variety of methods are available. The most elementary techniques are based on the equivalence between Ohm's and Kirchhoff's laws in electric networks and Darcy's law and the continuity equation in porous media flow. Well-known in this respect are the arithmetic and harmonic averages representing respectively the permeability parallel and normal to a sequence of rock layers. Renormalization techniques have been developed to successively upscale to coarser and coarser levels [15].

Homogenization may be considered as a sophisticated extension of these elementary techniques for arbitrary heterogeneous rocks [5,18,27,29] and has proved its effec-

tiveness for linear problems as they occur in single-phase porous media flow. In spite of some theoretical limitations of homogenization theory, practice shows that its range of applicability can be made much wider. However, since the average of a nonlinear function is not a nonlinear function of the average, the extension to nonlinear problems is far from trivial.

In this paper two-phase porous media flow is considered. The existing methods applied to upscale two-phase flow parameters can be roughly divided into two parts: (i) dynamic methods [3], also referred to as process-dependent methods, and (ii) steady-state methods [10,11,22,23], which we dub here ‘process independent methods’.

The process-independent approach is a way of upscaling of the two-phase capillary pressure and mobilities, in which the coarse-scale results obtained for a particular reservoir can be used in any simulation, irrespective of the scenario that is simulated. Process-independent coarse-scale functions can, therefore, be stored in databases to be retrieved for different types of study on the same reservoir or basin.

This is in contrast with process-dependent, or dynamic, upscaling, in which the coarse-scale capillary pressure and coarse-scale mobilities are optimally adapted to the scenario. These methods determine time-dependent coarse-scale parameters for each grid block. In fact, process-dependent upscaling may be considered as a kind of preconditioning to make the simulation computationally more efficient. The ‘dynamic upscaling approach’ leading to pseudo functions for each rock type has also gained popularity; see [3] for a review. Pseudo relative permeabilities are generally highly process dependent and thus their applicability is restricted to flow and parameter ranges very similar to those for which they were derived.

To facilitate the upscaling procedure, another group of methods has been developed. Here the basic assumption is that the flow is in steady state [10,11,22,23] and such methods fall into the category of process-independent upscaling. The method presented in this paper also belongs to this class of process-independent methods. This means that the coarse-scale capillary pressure and mobility functions – functions of the saturation – are time-independent. The approach we apply may be viewed as an extension of earlier-developed methods to numerically homogenize the absolute permeability for single-phase flow [27,29,30].

Our reasoning is based on the principle of *preservation of form*, stating that the mathematical form of the fine-scale equations should be preserved *as much as possible* on the coarse scale. This principle leads to the required extensions, while making the physics underlying homogenization transparent. It should be emphasized that from an engineering point of view it is of great importance to maintain the same form of upscaled equations. It is well known, however, that the ‘preservation of form’ argument fails with respect to the equation governing transport of dissolved mass through porous media [18].

One of the basic requirements for process-independent upscaling is that for a homogeneous medium the coarse-scale mobility function and the capillary pressure function are the same as the fine-scale functions. This result, which has also been postulated in [1,2], is what is intuitively expected from a homogenization method. Especially for

homogenization in the near well region, the principle of ‘conservation of homogeneity’ plays an important role [30].

In [10,11] the coarsening approach is presented to describe multiphase displacement. In this approach the homogenized parameters are obtained by direct use of the upscaled absolute permeability in conjunction with the fine-scale relative permeabilities. This is possible only when restricting to one set of relative permeability function (of the saturation) homogeneously throughout the flow domain. The method presented in this paper may be seen as an extension to heterogeneous relative permeability functions.

In the steady state upscaling presented by [22,23] two cases can be distinguished: (i) the capillary limit (capillary equilibrium), and (ii) the viscous limit. The ‘no-capillary gradient case’ discussed in this paper may be seen as similar to the viscous limit case.

The homogenization results [10,11,22,23] clearly show that the multiphase flow functions (capillary pressure and relative permeability as functions of the saturation) for the coarse scale are identical to those for the fine scale, even if the absolute permeability is heterogeneous. Hence, there is conservation of homogeneity.

The method presented in this paper is an extension of the above-mentioned results to more general cases of space-dependent capillary pressure and relative permeability functions.

In the method using higher moments to determine process-independent relative permeabilities [8], the off-diagonal components of the permeability have been neglected because general-purpose multiphase flow simulators handle permeability as a diagonal tensor. If the fine-scale permeability fields are correlated along coordinate directions such an approximation does not introduce a significant error. However, the off-diagonal terms may become significant when the fine scale permeability has a more complex spatial distribution. Therefore, the full tensor character of the mobilities has been taken into account in this paper.

As already stated, the study presented in this paper may be viewed as a continuation of our previous work on the homogenization of single-phase flow [27,29] and its extension to flow in near-well flow regions [30]. In this paper these methods are extended to two-phase flow, also in the near-well region. The coarse-scale parameter is computed through the solution of a local flow problem over fine scale region corresponding to the coarse grid block [12,16]. This problem is usually solved subject to mixed boundary conditions: linear pressure in the flow direction and no-flux boundaries perpendicular to the flow. This approach yields zero non-diagonal terms in the permeability matrix. However, in near well regions with highly heterogeneous permeability over small distances, anisotropy may play a role and, therefore, the side boundaries may not be closed. Here we consider the full tensor, also around wells.

The outline of the paper is as follows. Section 2 presents homogenization of two-phase porous media flow, emphasizing homogenization of the mobility and capillary pressure as nonlinear functions of the saturations. Section 3 gives some remarks relevant to the extension to homogenization of two-phase flow in the near-well region. In section 4 results of numerical experiments are presented. Finally, section 5 gives the summary and conclusions.

2. Homogenization of two-phase flow in porous media

2.1. Field equations for the cell problem

Here we consider incompressible two-phase flow in domain $\Omega \in \mathbb{R}^3$. Phases 1 and 2 are respectively the wetting phase (water) and the non-wetting phase (oil). The continuity equations for incompressible flow are [19]

$$\phi \partial_t s_\beta + \operatorname{div} \underline{q}_\beta = 0, \quad (1)$$

where ϕ is the porosity, \underline{q}_β is the flux density and s_β is the saturation of phase β ; the saturations satisfy the constraint $s_1 + s_2 = 1$.

Our derivation of the homogenization method is based on the principle of *preservation of form*. This principle requires that the equations on the coarse scale should, *as much as possible*, preserve their form on the coarse scale. At the same time, this requirement has strong implications for engineering practice. In reservoir engineering it is very desirable that the form of the coarse-scale equations is preserved; for example, to be able to apply commercially available simulation software that solves the fine-scale equations. As can be expected, preservation of form is not always possible, a notorious example being the equation describing transport of mass dissolved in groundwater. However, for the problems considered in this paper preservation of form is possible.

As a first step we require

$$\langle \operatorname{grad} f \rangle = \operatorname{grad} \langle f \rangle, \quad (2)$$

for any function $f(\underline{x})$. Requirement (2) is satisfied if the brackets $\langle \cdot \rangle$ denote the volume average over a *rectangular* cell $C(\underline{x}) \in \Omega$ centered at point $\underline{x} = \{x_1, x_2, x_3\}$ with volume $\Delta x_1 \Delta x_2 \Delta x_3$,

$$\langle f \rangle(\underline{x}) = \frac{1}{\Delta x_1 \Delta x_2 \Delta x_3} \iiint_{\underline{x}-\Delta \underline{x}/2}^{\underline{x}+\Delta \underline{x}/2} f(\underline{x}) \, dx_1 \, dx_2 \, dx_3. \quad (3)$$

Now we introduce an even stronger requirement: ‘The *fine-scale* formulation expressing the net volumetric outflow of a closed volume, $\operatorname{div} \underline{q}_\beta$, should have the *same form*, $\operatorname{div} \langle \underline{q}_\beta \rangle$, on the *coarse scale*.’ Expressed mathematically this means:

$$\operatorname{div} \underline{q}_\beta = \operatorname{div} \langle \underline{q}_\beta \rangle. \quad (4)$$

Let us define a ‘map position point’ $\underline{y} = \varepsilon \underline{x}$, where ε , the scale of the map, is a small number. Homogenization makes sense only if a variation of the fine-scale flux density \underline{q}_β over a real distance $\Delta \underline{x} = \underline{\ell}$ has the same order of magnitude as a variation of the coarse-scale flux density $\langle \underline{q}_\beta \rangle$ over the same distance $\Delta \underline{y} = \underline{\ell}$ on a map, i.e., over the much larger real distance $\Delta \underline{x} = \underline{\ell}/\varepsilon$. Hence the approximation of order zero to equation (4) written as $\partial q_{\beta i} / \partial x_i = \varepsilon \partial \langle q_{\beta i} \rangle / \partial y_i$ is [27]

$$\operatorname{div} \underline{q}_\beta = 0. \quad (5)$$

The classical homogenization approach – the ‘BLP approach’ [5] – represents a different heuristic towards the same homogenization procedure [27,29] and is based on multiscale asymptotic expansions. Since our approach – preservation of form – yields exactly the same results for the cases under consideration, our approach may be considered as an alternative that offers a physical interpretation of homogenization. Moreover, since the two heuristics lead to exactly the same results, the mathematical rigorousness of the BLP approach [5] in proving convergence when $\varepsilon \rightarrow 0$ remains valid in our approach.

Muskat’s extension of Darcy’s law [19] is

$$\underline{q}_\beta = -\underline{\lambda}_\beta \cdot \text{grad } \varphi_\beta. \quad (6)$$

For each phase β , $\underline{\lambda}_\beta$ is the mobility tensor, $\varphi_\beta = p_\beta - \rho_\beta \underline{g} \cdot \underline{x}$ is the scalar potential (briefly, the potential), p_β is the phase pressure and ρ_β is the phase density, while \underline{g} is the gravitational acceleration.

Since the medium is heterogeneous, the mobility has spatial fine-scale oscillations that cannot be accounted for in practical coarse-scale calculations. Therefore we want to solve the set of ‘equal form equations’ $\text{div } \underline{Q}_\beta = 0$, $\underline{Q}_\beta = -\underline{\Delta}_\beta \cdot \text{grad } \Phi_\beta$, where $\underline{\Delta}_\beta$, the coarse-scale mobility, is a properly defined average of $\underline{\lambda}_\beta$. Simple-minded averaging will not do. What does work is dissipation minimization:

$$\begin{aligned} & \underline{H}_\beta(\underline{x}) \cdot \underline{\Delta}_\beta(\underline{x}) \cdot \underline{H}_\beta(\underline{x}) \\ &= (\Delta x_1 \Delta x_2 \Delta x_3)^{-1} \\ & \times \inf \left\{ \iiint_{C(\underline{x})} \text{grad } \varphi_\beta(x') \cdot \underline{\lambda}_\beta(x' - x) \cdot \text{grad } \varphi_\beta(x') \, dV': \varphi_\beta \in \Phi(C; H_\beta) \right\}, \end{aligned}$$

where $\underline{H}_\beta(\underline{x})$ is a given 3D vector at the cell’s center \underline{x} and $\Phi(C; H_\beta)$ denotes the space of functions φ_β such that $\varphi_\beta(\underline{x}') + \underline{H}_\beta(\underline{x}')$ is a C -periodic function of \underline{x} , i.e., one that takes the same value at opposite points of the cell C . Based on the above formulation, convergence can be proved [5]. To find all nine components $\lambda_{\beta,ij}$ of the mobility tensor $\underline{\lambda}_\beta$, three linearly independent solutions $\varphi_{\beta,k}$, $k = 1, 2, 3$, obtained by three different sets of boundary conditions on the cell’s boundary ∂C (section 2.2), must be solved. Substitution of Darcy’s law (6) into continuity equation (5) yields the elliptic ‘div side equation’ [6]

$$\text{div}(\underline{\lambda}_\beta \cdot \text{grad } \varphi_{\beta,k}) = 0 \quad \text{in } C. \quad (7)$$

Since the flux density is solenoidal, we may use Poincaré’s lemma to introduce a vector potential $\underline{a}_{\beta,k}$ such that $\underline{q}_{\beta,k} = \text{rot } \underline{a}_{\beta,k}$. Using $\text{rot}(\text{grad } \varphi_{\beta,k}) \equiv \underline{0}$, we find the elliptic ‘curl side’ equation [6]

$$\text{rot}(\underline{\lambda}_\beta^{-1} \cdot \text{rot } \underline{a}_{\beta,k}) = \underline{0} \quad \text{in } C. \quad (8)$$

Now the coarse-scale mobility follows from (omitting index k)

$$\begin{aligned} & \underline{Q}_\beta(\underline{x}) \cdot \underline{\Delta}_\beta(\underline{x})^{-1} \cdot \underline{Q}_\beta(\underline{x}) \\ &= (\Delta x_1 \Delta x_2 \Delta x_3)^{-1} \\ & \times \inf \left\{ \iiint_{C(\underline{x})} \text{rot } \underline{a}_\beta(\underline{x}') \cdot \underline{\lambda}_\beta(\underline{x}' - \underline{x})^{-1} \cdot \text{rot } \underline{a}_\beta(\underline{x}') dV': \underline{a}_\beta \in \underline{A}(C; \varphi_\beta) \right\}, \end{aligned}$$

where $\underline{Q}_\beta(\underline{x})$ are given 3D vectors at the cell's center \underline{x} and $\underline{A}(C; \varphi_\beta)$ denotes the space of functions \underline{a}_β such that $\underline{a}_\beta(\underline{x}') - (1/2)\underline{Q}_\beta(\underline{x}')$ is a C -periodic vector function. Although equations (7) and (8) with their respective dissipation minimization principles are mathematically equivalent, they lead to different discrete analogs [6], respectively the conformal-nodal finite element method and the mixed-hybrid finite element method. This allows us to assess bilateral error bounds for the eigenvalues of the coarse-scale mobility tensors [27].

2.2. Periodic boundary conditions for the cell problem

To find three different solutions of equations (7) and (8), we use boundary conditions that specify constant potential differences between two 'equivalent points' on opposite boundaries of the homogenization cell C [5]. The boundary condition for the scalar potential is

$$\varphi_{\beta,i} \left(x_j + \frac{1}{2} \Delta x_j, \cdot, \cdot \right) - \varphi_{\beta,i} \left(x_j - \frac{1}{2} \Delta x_j, \cdot, \cdot \right) = -H_{\beta,ij} \Delta x_j \quad \text{on } \partial C, \quad (9)$$

(no summation over index j) and an analog for the vector potential may be used too. As a consequence, the potential may be written as $\varphi_{\beta,i}(\underline{x}) = \chi_{\beta,i}(\underline{x}) - \underline{H}_{\beta,i} \cdot \underline{x}$ with periodic $\chi_{\beta,i}(\underline{x})$ and constant $\underline{H}_{\beta,i}$. Hence, the capillary pressure $p_{2,i} - p_{1,i}$ is equal to a periodic 'capillary potential' φ_i plus a linear trend $\underline{L}_i \cdot \underline{x}$, such that $\underline{H}_{2,i} - \underline{H}_{1,i} = (\rho_1 - \rho_2)\underline{g} - \underline{L}_i$. The flux densities $\underline{q}_{\beta,i}$ and negative potential gradients $\underline{h}_{\beta,i} = -\text{grad}\varphi_{\beta,i}$ are periodic with constant volume averages

$$\langle \underline{q}_{\beta,i} \rangle = \text{rot} \left(\frac{1}{2} \underline{Q}_{\beta,i} \times \underline{x} \right) = \underline{Q}_{\beta,i} \quad \text{and} \quad \langle \underline{h}_{\beta,i} \rangle = \text{grad}(\underline{H}_{\beta,i} \cdot \underline{x}) = \underline{H}_{\beta,i},$$

respectively.

Choosing boundary conditions (9) such that $\underline{H}_{1,i} \neq \underline{H}_{2,i}$ means that we take the influence of gravity or a linear trend of the capillary pressure into account in the homogenization procedure. When doing so, we find that a *homogeneous* capillary function of the saturation $p_{2,i} - p_{1,i} = p(s_1)$ combined with *homogeneous* mobilities $\underline{\lambda}_1(s_1), \underline{\lambda}_2(s_2)$ (section 2.3) does not yield the same functions on the coarse scale. Since this contradicts the principle of 'conservation of homogeneity', we assume $\underline{H}_{1,i} = \underline{H}_{2,i} = \underline{H}_i$. (In section 3 a similar argument is used to homogenize a near-well region.) This assumption makes it possible to introduce the following choice [5]

$$H_{ij} = \delta_{ij} \quad (\text{component } j \text{ of vector } i). \quad (10)$$

Preservation of form requires that Darcy's law on the fine scale should be preserved on the coarse scale, i.e.,

$$\langle \underline{q}_{\beta,i} \rangle = -\underline{\Lambda}_{\beta} \cdot \text{grad} \langle \varphi_{\beta,i} \rangle. \quad (11)$$

Using requirement (2), boundary condition (9) and choice (10) in equation (1) yields a simple expression for the coarse-scale mobility tensor $\underline{\Lambda}_{\beta}$ [18]:

$$\Lambda_{\beta,ij} = -\langle \underline{q}_{\beta,i} \rangle_j \quad (\text{component } j \text{ of solution } i). \quad (12)$$

Requirement (4) for $\underline{q}_{\beta,i}$ can be multiplied by φ_{β} and integrated over C . Using Gauss's divergence theorem and the periodicity assumption shows that the volume averaged dissipation tensor is equal to the coarse-scale dissipation tensor [29].

$$\langle \text{grad} \varphi_{\beta,i} \cdot \underline{\lambda}_{\beta} \cdot \text{grad} \varphi_{\beta,j} \rangle = \text{grad} \langle \varphi_{\beta,i} \rangle \cdot \underline{\Lambda}_{\beta} \cdot \text{grad} \langle \varphi_{\beta,j} \rangle. \quad (13)$$

Again using equations (2), (9) and (10), expression (13) yields [5]

$$\Lambda_{\beta,ij} = -\langle \text{grad} \varphi_{\beta,i} \cdot \underline{q}_{\beta,j} \rangle. \quad (14)$$

Since the fine-scale mobilities are symmetric [7], it follows from equation (13) that the coarse-scale mobilities are symmetric too. Thanks to the periodicity, the well-known fine-scale forms of *both* Darcy's law *and* the dissipation equation are preserved on the coarse scale as respectively state equations (11) and (13).

2.3. Constitutive equations

The mobilities are generally written as $\underline{\lambda}_{\beta}(\underline{x}, s_{\beta}) = \mu_{\beta}^{-1} r_{\beta}(\underline{x}, s_{\beta}) \underline{k}(\underline{x})$, where $\underline{k}(\underline{x})$ is the absolute permeability tensor, $r_{\beta}(\underline{x}, s_{\beta})$ is the relative permeability and μ_{β} is the viscosity of phase β [19]. It is assumed that the fine-scale relative permeabilities are scalar functions, but this scalar character will generally be lost on the coarse scale. This way, equations (7) and (8) are *independent* of the viscosities.

It is also generally assumed that the capillary pressure is a function of the saturation, i.e., $p_2 - p_1 = p(\underline{x}, s_1)$. Phases 1 and 2 are respectively the wetting and non-wetting phase, with $\partial p / \partial s_1 \leq 0$ [19]. Since boundary conditions (9) are specified for potential *differences*, the potentials are unique up to an arbitrary constant. Therefore, it makes sense to define the capillary potential as

$$\varphi_i = \varphi_{2,i} - \varphi_{1,i} + \langle \varphi_{1,i} \rangle - \langle \varphi_{2,i} \rangle + P, \quad (15)$$

where P is a specified *constant*. This capillary potential is equated to the capillary pressure

$$p(\underline{x}, s_{1,i}) = \varphi_i(\underline{x}). \quad (16)$$

In any point \underline{x} equation (16) is an implicit nonlinear equation for the saturation $s_{1,i}$, which we solve using the bisection method [24]. For each specified coarse-scale capillary pressure $\langle \varphi_i \rangle = P$, the coarse-scale saturations follow from $S_{\beta,i} = \langle \phi s_{\beta,i} \rangle / \langle \phi \rangle$,

yielding three coarse-scale capillary pressure functions $P(S_{1,i})$, $i = 1, 2, 3$. In most practical cases, these three functions can be approximated by only one capillary pressure function (see below). The determination of the coarse-scale capillary pressure function $P(S_1)$ is considered as an essential part of the process-independent homogenization approach discussed in this paper.

The coarse-scale mobilities can be determined by conventional numerical homogenization techniques based on solving the elliptic equations (7) or (8) [25,27,29]. Here these equations are solved by finite element methods, while the coupling between the two phases is done by successive substitutions.

2.3.1. Zero capillary pressure gradient

The ‘no-capillary-gradient’ approximation $\text{grad}(\varphi_{2,i} - \varphi_{1,i}) = \underline{0}$ can often be justified, notably in the near-well region, where the potential gradients are large. However, the no-capillary-gradient case plays also a role in the numerical algorithm. If the capillary pressure gradient vanishes, equations (7) and (8) have solutions only if $\nu \mu_1 \underline{\lambda}_1 = \mu_2 \underline{\lambda}_2$ for some specified constant $\nu \geq 0$, yielding

$$\frac{r_2(\underline{x}, 1 - s_1)}{r_1(\underline{x}, s_1)} = \nu \quad (\nu \text{ is a specified constant}). \quad (17)$$

In any point \underline{x} equation (17) is an implicit nonlinear equation for the saturation s_1 , here solved using the bisection method [24]. It follows from equation (17) that $S_{\beta,1} = S_{\beta,2} = S_{\beta,3} = S_\beta$, independent of the choice of boundary conditions.

2.3.2. Nonzero capillary pressure gradient

In cases where the capillary pressure gradient does not vanish, the saturations obtained from the no-capillary-gradient case are used as initial values in the iteration process by successive substitutions. Since the coarse-scale capillary gradient $\text{grad} P$ is equal to zero in the homogenization cell C , we may expect that nonzero fine-scale capillary gradients do not cause large deviations from the initial saturations that follow from equation (17). Hence the differences between $S_{\beta,1}$, $S_{\beta,2}$ and $S_{\beta,3}$ will be small, yielding only one capillary pressure function $P(S_1)$ as a good approximation.

2.4. Coarse-scale equations

Equations (11) and (13) are respectively the coarse-scale Darcy’s law and dissipation equation. According to requirement (2), averaging of the fine-scale continuity equations (1) yields

$$\langle \phi \partial_t s_\beta \rangle + \text{div} \langle \underline{q}_\beta \rangle = 0. \quad (18)$$

Under the assumption that the porosity ϕ is time-independent, substitution of requirement (3) into equation (18) and using equation (1) yields

$$\partial_t (\phi s_\beta - \langle \phi s_\beta \rangle) = 0, \quad (19)$$

expressing that the spatially fluctuating fine-scale void fractions ϕs_β are changing in time with the same rate as the spatially much smoother coarse-scale void fractions $\langle \phi s_\beta \rangle$. The total volume of phase β in homogenization cell C is $V_\beta = \langle \phi s_\beta \rangle \Delta x_1 \Delta x_2 \Delta x_3$ and since $V_1 + V_2 = \langle \phi \rangle \Delta x_1 \Delta x_2 \Delta x_3$, equation (19) yields $\phi \partial_t s_\beta = \langle \phi \rangle \partial_t S_\beta$ with $S_\beta = \langle \phi s_\beta \rangle / \langle \phi \rangle$, $S_1 + S_2 = 1$. Hence, defining $\Phi = \langle \phi \rangle$, the coarse-scale continuity equations are

$$\Phi \partial_t S_\beta + \operatorname{div} \langle \underline{q}_\beta \rangle = 0, \quad (20)$$

which preserve indeed the form of the fine-scale expression (1).

3. Homogenization of the near-well region

The results obtained in section 2 can be generalized to homogenization in a near-well region, where the upscaling cell is the segment of a circular cylinder. Transitions from finer to coarser scales are often based on volume-averaging theorems that convert integrals of the differential operators ∂_t , div , rot , grad of a function to the same differential operators working on the integrals of that function, plus integrals over the cell's boundary [13]. For random media the upscaling cell is the 'representative elementary volume' [4], while for periodic media the cell is the 'periodicity volume' [5]. Indeed, in section 2 we have exemplified that homogenization is equivalent with volume averaging for periodic cells.

However, the requirement that upscaling should be based on volume averaging sets too strict limits. Considering upscaling in the near-well region as an example, we will show that coarse-scale equations need not necessarily be relations between the *volume-averaged* fine-scale potential and flux density. It suffices to dispose of equations that relate coarse-scale *approximations* of those fine-scale quantities [28]. Allowing for this relaxation, the principle of preservation of form can be used to applications outside the scope of classical volume-averaging and homogenization theory [30].

3.1. Transformation to rectangular cell

The homogenization cell $C \in \mathbb{R}^3$ around the well is no longer rectangular, but has the form of a circular or elliptic cylinder. First, we define curvilinear orthogonal coordinates \tilde{x}_i with metrical coefficients m_i [17]. The cell's boundaries are then the curved planes $\tilde{x}_i = \text{constant}$. For instance, a circular cylindrical cell with outer radius R_C around a well with radius R_W is described using the well-known circular cylinder coordinates $R_W \leq \tilde{x}_1 = r \leq R_C$, $0 \leq \tilde{x}_2 = \theta < 2\pi$, $\tilde{x}_3 = z$ with metrical coefficients $m_1 = 1$, $m_2 = r$, $m_3 = 1$ [17].

Accepting other approximations than *volume-averages*, the proper choice for the averaging operator is

$$\langle f \rangle = \frac{1}{\Delta \tilde{x}_1 \Delta \tilde{x}_2 \Delta \tilde{x}_3} \iiint_{\tilde{C}} f(\tilde{x}'_1, \tilde{x}'_2, \tilde{x}'_3) d\tilde{x}'_1 d\tilde{x}'_2 d\tilde{x}'_3, \quad (21)$$

where the integration is from $\tilde{x}_i - (1/2)\Delta\tilde{x}_i$ to $\tilde{x}_i + (1/2)\Delta\tilde{x}_i$ (note the analogy with equation (3)). It is important to note that average (21) satisfies the form preservation requirement (2), $\langle \partial f / \partial \tilde{x}_i \rangle = \partial \langle f \rangle / \partial \tilde{x}_i = \Delta \bar{f} / \Delta \tilde{x}_i$, where \bar{f} is an average over the surface area of a boundary. By this construction, the upscaling method will relate the *pressure difference* $\Delta \bar{p}$ between the well screen and the outer boundary of the cell to the discharge rate Q into the well [30]. The near-well pressure difference and the well's discharge rate are the quantities of interest in engineering applications [9,12,20,21,26], rather than the volume averaged pressure gradients and volume averaged flux densities derived from using volume averaging and homogenization techniques indiscriminately.

Let us define the transformed flux density $\tilde{q}_i = m_1 m_2 m_3 q_i / m_i$ and the mobility $\tilde{\lambda}_{ij} = m_1 m_2 m_3 \lambda_{ij} / m_i m_j$. (In this section there is *no* summation over repeated indices.) Then the analogs of equations (5) and (6) are

$$\sum_{i=1}^3 \frac{\partial \tilde{q}_i}{\partial \tilde{x}_i} = 0 \quad (\text{continuity}), \quad (22)$$

$$\tilde{q}_i = - \sum_{j=1}^3 \tilde{\lambda}_{ij} \frac{\partial \varphi}{\partial \tilde{x}_j} \quad (\text{Darcy's law}). \quad (23)$$

It is observed that equations (22), (23) written in curvilinear orthogonal $\tilde{x}_1 \tilde{x}_2 \tilde{x}_3$ coordinates have exactly the same form as the continuity equation and Darcy's law in Cartesian coordinates. However, here the cylindrical homogenization cell C around the well has been transformed to a rectangular cell \tilde{C} with 'volume analog' $\Delta \tilde{x}_1 \Delta \tilde{x}_2 \Delta \tilde{x}_3$, which gives rise to the *transformed* flux density and mobility. Hence, the homogenization procedure is the same as described in section 2 for the far field.

3.2. Back transformation to original cell

Thus far, we have been able to use classical homogenization theory to determine the *transformed* homogenized mobility $\tilde{\underline{\underline{\Lambda}}}$ in the transformed cell \tilde{C} . However, we are interested in the coarse-scale mobility $\underline{\underline{\Lambda}}$ as it occurs in the original homogenization cell C around the well. Hence, we introduce a back transform from $\tilde{\underline{\underline{\Lambda}}}$ to $\underline{\underline{\Lambda}}$.

To this end, we invoke the principle of 'conservation of homogeneity', as introduced in section 1. Let us consider a *homogeneous* medium with fine-scale mobility $\underline{\underline{\lambda}}^{(c)}$. For this homogeneous medium the above homogenization procedure yields a transformed homogenized mobility $\tilde{\underline{\underline{\Lambda}}}^{(c)}$. Now the homogeneous fine-scale mobility $\underline{\underline{\lambda}}^{(c)}$ for which $\tilde{\underline{\underline{\Lambda}}}^{(c)} = \tilde{\underline{\underline{\Lambda}}}_{ij}$ is considered as the coarse-scale mobility $\underline{\underline{\Lambda}}$. Thus the back transform is equivalent to solving the following system of algebraic equations

$$\tilde{\underline{\underline{\Lambda}}}_{ij}^{(c)} (\Lambda_{11}, \Lambda_{12}, \dots, \Lambda_{32}, \Lambda_{33}) - \tilde{\underline{\underline{\Lambda}}}_{ij} = 0, \quad (24)$$

which, in the general case, need to be solved numerically. Here a Newton–Raphson method was applied.

At this stage it is appropriate to position our approach in the wider scope of research activities presented in the literature. The coarse-scale parameter is computed through the solution of a local flow problem over the fine-scale region corresponding to the coarse grid block [12,16]. This problem is usually solved subject to mixed boundary conditions: linear pressure in the direction of flow to the well – for instance, periodic or constant pressure difference – and no flux in the other directions. This approach leads to a neglect of the off-diagonal terms in the mobility matrices. However, especially when the permeability field is highly variable over small distances, anisotropy may play a role. To account for this, our approach extends the methods presented in the literature by the introduction of less constraining boundary conditions. This gives the flow more freedom to flow according to heterogeneities in the mobilities, rather than to flow along boundary constraints. This will finally result in mobility tensors taking the full anisotropy into account.

4. Numerical examples

This section is devoted to numerical examples illustrating the above-presented theories. The results have been obtained using the *two* complementary methods: the conformal-nodal finite element method (CN-FEM) and the mixed-hybrid finite element method (MH-FEM) [14]. The two methods approximate the unique solution of a partial differential equation. However, they do so in algebraically different ways, such that they provide bilateral error bounds for the eigenvalues of the homogenized mobility tensor, see [27] for a formal proof. As will be shown below, these theoretical bounds are reflected in our numerical results: The eigenvalues of the coarse-scale mobility tensor obtained by CN-FEM are always greater than the eigenvalues obtained by MH-FEM. However, here we have used *continuous* fine-scale mobilities to define the ‘original problem’, from which we derived a sequence of different discrete problems. Therefore, the exact solution of the continuous problem will not necessarily lie in between the two numerical solutions. Only problems in which the fine-scale permeability is piecewise constant from the beginning have solutions that are bounded by CN-FEM and MH-FEM, as has been shown in [27,29,30]. Nevertheless, solving problems for continuous mobilities using two different numerical methods may be considered as a validation of the quality of the approximation.

The section is divided into two subsections: homogenization of mobilities and capillary pressure in the far field (section 4.1) and homogenization in the near-well region (section 4.2).

4.1. Homogenization of mobilities and capillary pressure

Let us consider an isotropic porous medium with absolute permeability

$$k(\underline{x}) = \zeta(\underline{x}) \times 10^{-3} \mu\text{m}^2 \quad (1 \mu\text{m}^2 = 1013.250 \text{ mD}),$$

where

$$\zeta(x, y, z) = 8\eta^{-1}\alpha\beta\gamma \cosh^2 x \cos^2 y \cosh^2 z$$

in the domain $|x| \leq \alpha$, $|y| \leq \beta$, $|z| \leq \gamma$. Outside this domain the function $\zeta(\underline{x})$ is continued periodically. The factor $\eta = (\alpha + \frac{1}{2} \sinh 2\alpha)(\beta + \frac{1}{2} \sin 2\beta)(\gamma + \frac{1}{2} \sinh 2\gamma)$ is chosen such that $\langle \zeta \rangle = 1$ and $\langle \zeta^{-1} \rangle = 8^{-1}(\alpha\beta\gamma)^{-2} \mu \tanh \alpha \tan \beta \tanh \gamma$. The water has viscosity $\mu_1 = 5 \times 10^{-4}$ Pa·s = 0.5 cp, while the oil has viscosity $\mu_2 = 5 \times 10^{-2}$ Pa·s = 50 cp. The relative permeabilities are $r_1(s_1) = \frac{2}{3}(s_1^{2\zeta(\underline{x})} - (\frac{1}{10})^{2\zeta(\underline{x})})$ and $r_2(s_2) = \frac{8}{7}(s_2^{2\zeta(\underline{x})} - (\frac{1}{5})^{2\zeta(\underline{x})})$. The capillary pressure is given by $p(\underline{x}, s_1)/p_0 = b \tan((9 - 20s_1)\pi/14) + d(\underline{x})$ ($p_0 = 1$ kPa = 0.1450377 psi), where either $b = 0$ and d is constant (the no-capillary gradient case) or $b = 1$ and $d(\underline{x}) = 5\zeta(\underline{x})^{-1}/2$ (the saturation-dependent capillary case). The admissible interval for the water saturation is $\frac{1}{10} \leq s_1 \leq \frac{4}{5}$; the residual oil saturation is $\frac{1}{5}$ and the maximum oil saturation is $\frac{9}{10}$. In this example the exact coarse-scale absolute permeability \underline{K} can be determined analytically and is given by the diagonal matrix

$$\text{diag}(K_{xx}, K_{yy}, K_{zz}) = \text{diag}(F_x, F_y, F_z) \times 10^{-3} \mu\text{m}^2,$$

where

$$F_x = \frac{2\alpha^2 \coth \alpha}{\alpha + (1/2) \sinh 2\alpha}, \quad F_y = \frac{2\beta^2 \cot \beta}{\beta + (1/2) \sin 2\beta} \quad \text{and} \quad F_z = \frac{2\gamma^2 \coth \gamma}{\gamma + (1/2) \sinh 2\gamma}$$

[27,29]. In the finite element analogs, where the fine-scale mobility is tetrahedron-wise constant, we assign to each tetrahedron the fine-scale mobility using the above expressions in its barycenter. In the numerical examples we have chosen $\alpha = \gamma = 49/50$ and $\beta = (49/50) \times \pi/2$.

To perform the numerical experiments, the following nine values of ν have been specified: 0.0001, 0.0003, 0.001, 0.01, 0.1, 1, 10, 100, 300. Then, equation (17) is solved

Coarse-scale water saturation

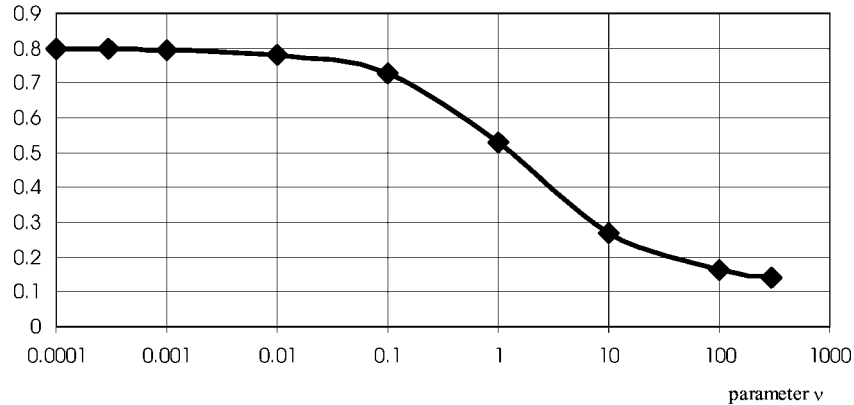


Figure 1. Coarse-scale water saturation S_1 vs. ratio of fine-scale relative permeabilities ν .

numerically using the bisection method with termination criterion $|r_2(s_2)/r_1(s_1) - \nu| \leq 10^{-8}$ yielding the coarse-scale saturations for each specified ν (figure 1) from which the corresponding mobilities are calculated.

The numerical homogenization has first been performed for the no-capillary-gradient case ($b = 0, d = \text{constant}$). A tetrahedral mesh consisting of $N = 26 \times 26 \times 26 = 17576$ active nodes was used. The results for this case, which hold for any constant capillary pressure, are shown in table 1. Because of the symmetry in the directions x and z only results obtained for the x direction are reported and plotted.

These values, together with the results obtained with the mixed-hybrid finite element method, are summarized in graphical form in figures 2 and 3. In the pictures presented below Lxx-MH means Λ_{xx}^w computed by mixed-hybrid finite elements, while Lxx-CN means Λ_{xx}^w computed by conformal-nodal finite elements, and similarly for Lyy.

Table 1
No capillary gradient; CN-FEM: $N = 26 \times 26 \times 26$.

ν	S_1	$\Lambda_{1,xx}$	$\Lambda_{1,yy}$	$\Lambda_{2,xx}$	$\Lambda_{2,yy}$
0.0001	0.79916	6.2318E-01	2.5165E-02	6.2317E-07	2.5164E-08
0.0003	0.79819	6.1724E-01	2.5159E-02	1.8517E-06	7.5485E-08
0.001	0.79592	6.0512E-01	2.5145E-02	6.0516E-06	2.5148E-07
0.01	0.78193	5.4931E-01	2.5050E-02	5.4930E-05	2.5050E-06
0.1	0.72773	4.1973E-01	2.4463E-02	4.1973E-04	2.4463E-05
1	0.53142	2.2063E-01	1.8569E-02	2.2063E-03	1.8569E-04
10	0.26714	5.8242E-02	3.1125E-03	5.8242E-03	3.1125E-04
100	0.16490	9.3643E-03	3.2276E-04	9.3643E-03	3.2276E-04
300	0.14097	3.5730E-03	1.0802E-04	1.0719E-02	3.2406E-04

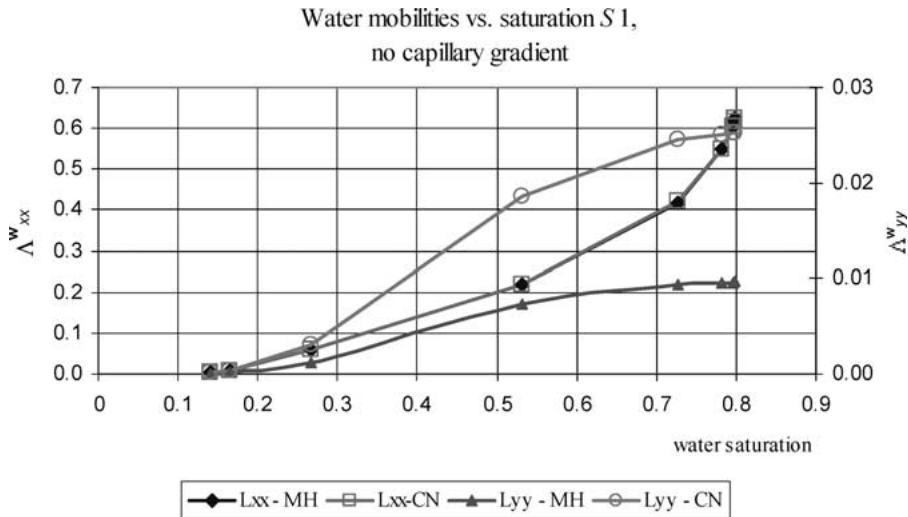


Figure 2. Coarse-scale water mobilities $\Lambda_{ij}^w = \Lambda_{1,ij}$ vs. coarse-scale water saturation S_1 .

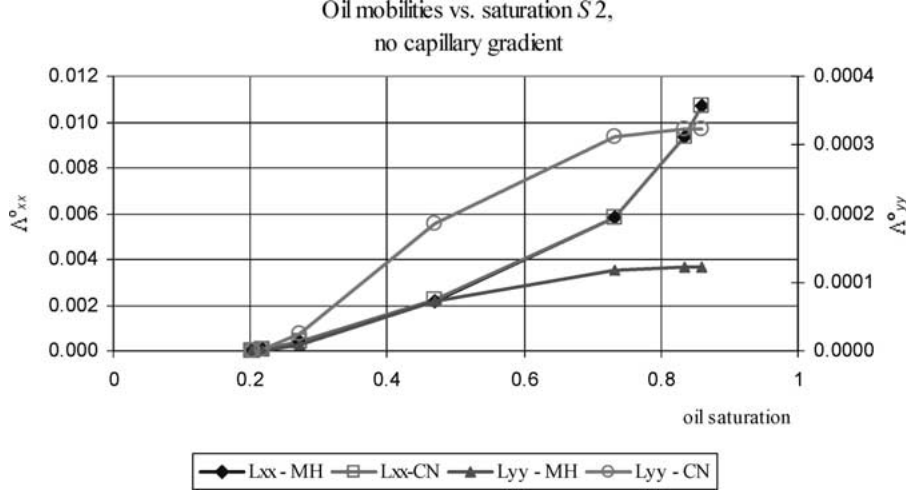


Figure 3. Coarse-scale oil mobilities $\Lambda_{ij}^o = \Lambda_{2,ij}$ vs. coarse-scale oil saturation S_2 .

Table 2
Saturation dependent capillary; CN-FEM: $N = 26 \times 26 \times 26$.

P	S_1	$\Lambda_{1,xx}$	$\Lambda_{1,yy}$	$\Lambda_{2,xx}$	$\Lambda_{2,yy}$
-3875.4000	0.79994	6.2921E-01	2.5169E-02	2.8502E-07	5.0005E-08
-1278.6000	0.79983	6.2895E-01	2.5167E-02	8.6262E-07	1.4549E-07
-368.2400	0.79942	6.2800E-01	2.5161E-02	2.9709E-06	4.4256E-07
-16.6780	0.79017	6.0295E-01	2.5101E-02	5.4448E-05	2.3545E-06
18.7980	0.22428	6.8110E-03	2.2250E-03	1.3948E-02	4.5301E-06
22.8390	0.20969	4.8853E-03	1.7742E-03	1.4085E-02	5.0936E-06
25.3930	0.20263	4.0890E-03	1.5709E-03	1.4146E-02	5.5635E-06
44.7540	0.17083	1.6570E-03	8.2975E-04	1.4368E-02	3.6480E-05
86.9900	0.14819	6.9004E-04	3.9232E-04	1.4497E-02	1.8273E-04

To solve the saturation-dependent capillary case ($b = 1$, $d(\underline{x}) = 5\zeta(\underline{x})^{-1}/2$), the saturations obtained from the no-capillary-gradient case have been chosen as initial values for the successive iteration procedure.

It is recalled here that for the homogenization three numerical solutions must be determined. Hence, each solution has its own coarse-scale saturations $S_{\beta,i}(P)$. However, it turns out that $S_{\beta,1}$, $S_{\beta,2}$ and $S_{\beta,3}$ do not deviate much from the average $S_{\beta} = \frac{1}{3}(S_{\beta,1} + S_{\beta,2} + S_{\beta,3})$; the largest difference was 0.0002. Moreover, the coarse-scale saturations obtained with the two finite element methods were equal.

The results obtained for the saturation-dependent capillary pressure are shown in table 2. Only values obtained with CN-FEM are reported. Results obtained with the two methods are summarized in figures 4–6.

In this example the coarse-scale relative permeabilities are $\text{diag}(R_{\beta,xx}, R_{\beta,yy}, R_{\beta,zz}) = \mu_{\beta} \text{diag}(F_x^{-1} \Lambda_{\beta,xx}, F_y^{-1} \Lambda_{\beta,yy}, F_z^{-1} \Lambda_{\beta,zz})$, which can generally be handled by con-

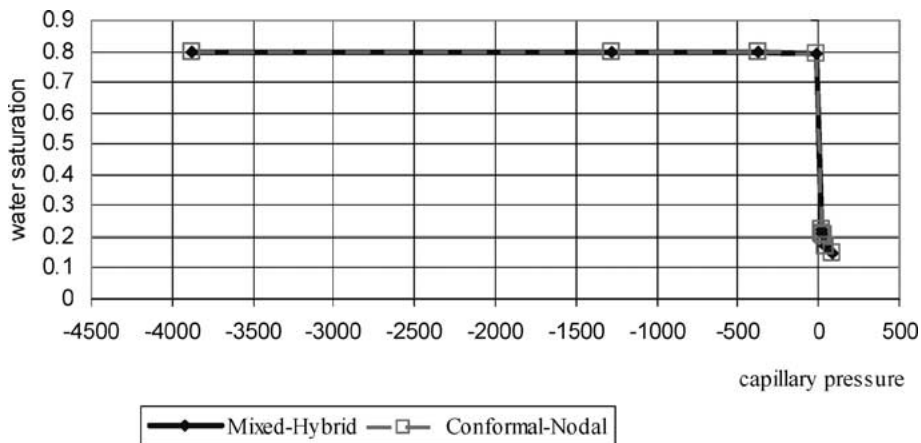


Figure 4. Coarse-scale water saturation S_1 vs. coarse-scale capillary pressure P .

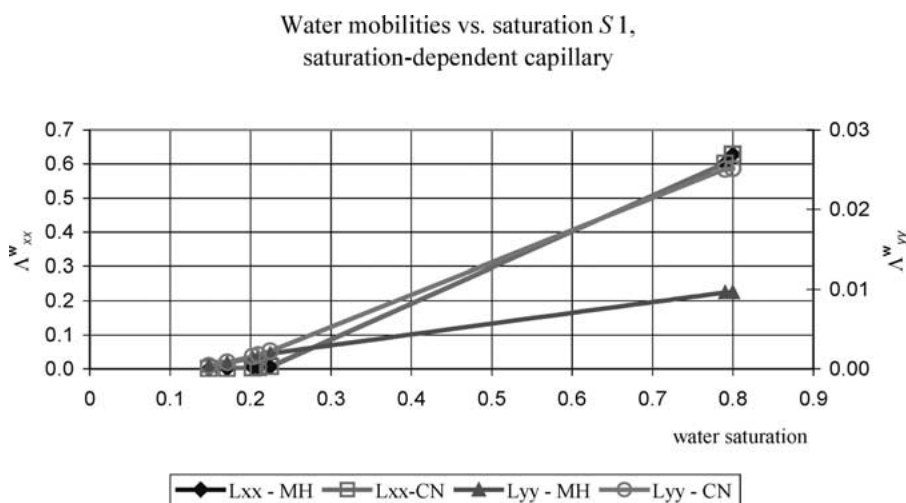


Figure 5. Coarse-scale water mobilities $\Lambda_{ij}^w = \Lambda_{1,ij}$ vs. coarse-scale water saturation S_1 .

ventional reservoir simulators. The diagonal form of the coarse-scale permeabilities is due to the same heterogeneity pattern η of the fine-scale permeability and the capillary pressure and, moreover, to the mirror symmetries in the ‘heterogeneity function’ $\eta(x, y, z) = \eta(\pm x, \pm y, \pm z)$.

Since we have access to two algebraically different approximation methods to solve the problem, there is a temptation to compare their behavior. Thus, a set of computational experiments has been performed aiming to study the two approximate solutions. The parameter value $\nu = 0.1$ has been chosen for that purpose. The computations were performed for a sequence of uniformly refined meshes. The results are summarized in figures 7–12.

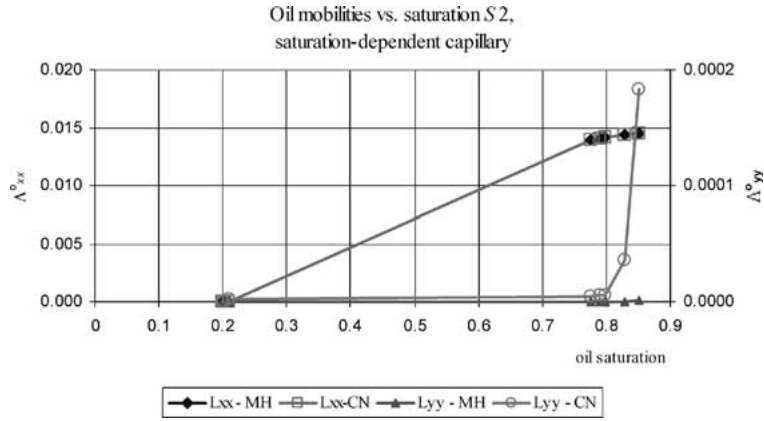


Figure 6. Coarse-scale oil mobilities $\Lambda_{ij}^o = \Lambda_{2,ij}$ vs. coarse-scale oil saturation S_2 .

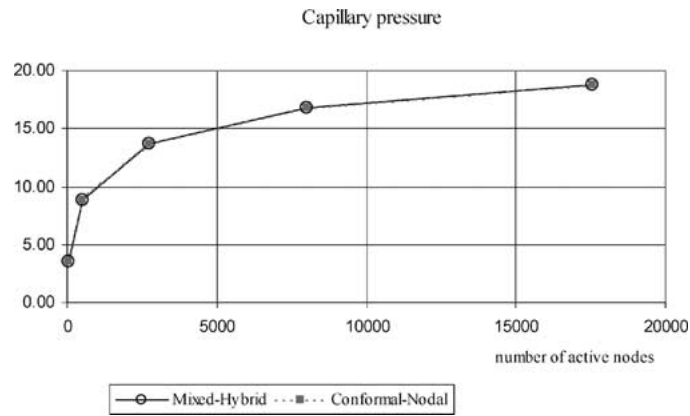


Figure 7. Coarse-scale capillary pressure vs. number of active nodes.

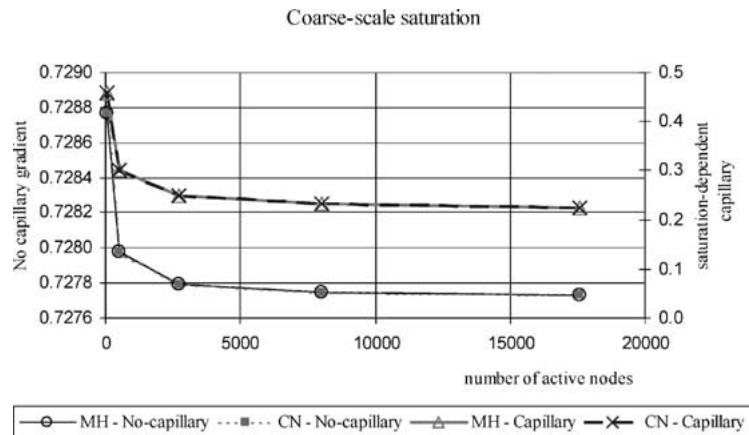


Figure 8. Coarse-scale water saturation vs. number of active nodes.

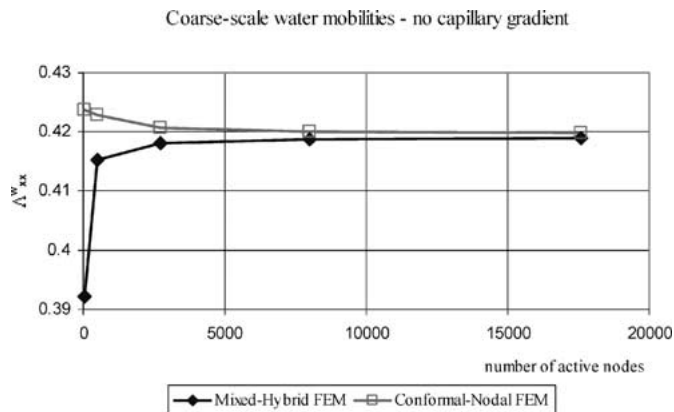


Figure 9. No capillary gradient: coarse-scale water mobilities $\Lambda_{xx}^w = \Lambda_{1,xx}$ vs. number of active nodes.

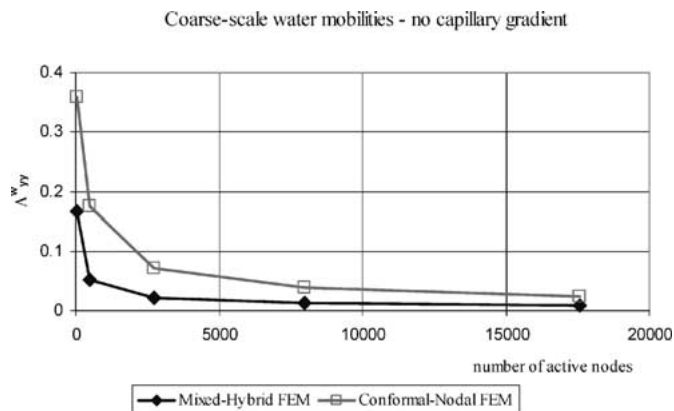


Figure 10. No capillary gradient: coarse-scale water mobilities $\Lambda_{yy}^w = \Lambda_{1,yy}$ vs. number of active nodes.

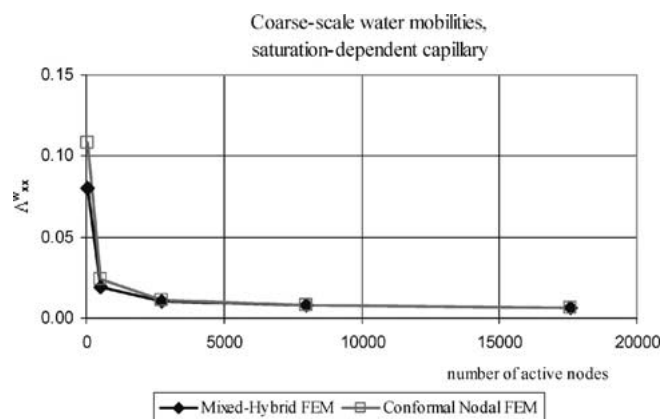


Figure 11. Saturation-dependent capillary: coarse-scale water mobilities $\Lambda_{xx}^w = \Lambda_{1,xx}$ vs. number of active nodes.

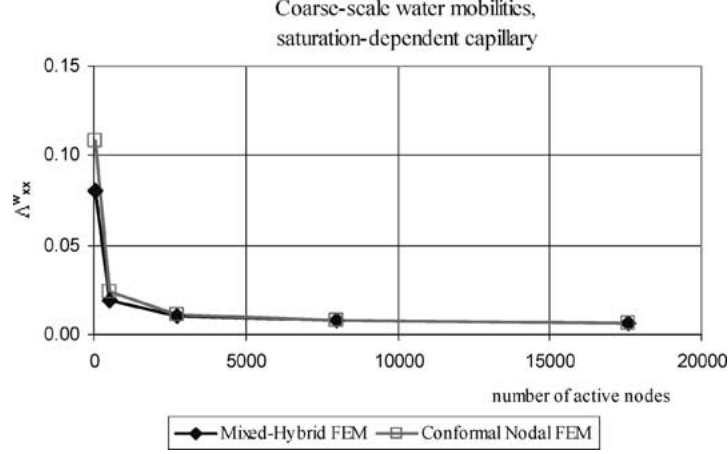


Figure 12. Saturation-dependent capillary: coarse-scale water mobilities $\Lambda_{yy}^w = \Lambda_{1,yy}$ vs. number of active nodes.

The two methods provide solutions that are very close to each other. In general, the differences in the yy component between two solutions are greater. This is due to the form of the fine-scale absolute permeability, which is steeply descending to zero near the y -boundaries.

The function describing the fine-scale absolute permeability is continuous, while the two finite-element methods use tetrahedron-wise constant fine-scale mobility values. Hence, for each mesh in the sequence of meshes used in the computations another discrete problem is derived from the continuous problem. For each problem in the sequence of discrete problems, the CN-FEM and MH-FEM solutions represent respectively the upper and lower bounds. However, the exact solution of the continuous problem is not bounded by the CN-FEM and MH-FEM solutions presented here.

4.2. Homogenization in the near-well region

The homogenization method illustrated in section 4.1 can straightforwardly be extended to homogenization in the near-well region [27,30]. As an example, we consider an *anisotropic* porous medium of which the diagonal matrix

$$\text{diag}(k_{rr}, k_{\theta\theta}, k_{zz}) = \text{diag}(r^{-1}, r, r^{-1})\zeta(r - \alpha - R_W, \theta, z) \times 10^{-3} \mu\text{m}^2$$

gives the absolute permeability, where $\zeta(r, \theta, z)$ is the same function as in section 4.1. However, in this case the periodic continuation in the θ -direction is such that the segments $149\pi < 100\theta \leq 150\pi$, $-50\pi < 100\theta < -49\pi$ and $49\pi < 100\theta < 51\pi$ have a sufficiently high mobility to cause that the homogenization intervals $-49\pi \leq 100\theta \leq 49\pi$ and $51\pi \leq 100\theta \leq 149\pi$ are ‘directly neighboring’ to each other. In our experiments we have chosen a well radius $R_W = 4/100$; then the cell radius is $R_C = 2\alpha + R_W = 2$. Again, the mesh consisting of $N = 26 \times 26 \times 26$ active nodes was used.

Table 3

Back transform of the transformed coarse-scale mobilities; CN-FEM: $N = 26 \times 26 \times 26$.

S_1	$\tilde{\Lambda}_{1xx}$	$\tilde{\Lambda}_{1yy}$	Λ_{1rr}	$\Lambda_{1\theta\theta}$	Λ_{1zz}
No-capillary gradient case					
0.75186	0.46699	9.53E-03	9.10E-01	4.85E-03	4.58E-01
0.53142	0.22016	7.28E-03	4.29E-01	3.70E-03	2.16E-01
0.26714	5.81E-02	1.18E-03	1.13E-01	5.99E-04	5.70E-02
0.14097	3.57E-03	4.04E-05	6.95E-03	2.06E-05	3.50E-03
Saturation dependent capillary					
0.79017	0.60237	9.62E-03	1.17E+00	4.89E-03	5.91E-01
0.25696	1.27E-02	2.86E-03	2.46E-02	1.46E-03	1.24E-02
0.14819	6.62E-04	3.76E-04	1.29E-03	1.91E-04	6.49E-04

In this simple example, the transformed absolute permeabilities are isotropic with $\tilde{k}_{xx} = \tilde{k}_{yy} = \tilde{k}_{zz} = \zeta(\tilde{x}, \tilde{y}, \tilde{z}) \times 10^{-3} \mu\text{m}^2$. Also for the viscosities, relative permeabilities and capillary pressure we take the same functions as in section 4.1. This way the homogenization is exactly the same as in section 4.1, except that now a back transformation of the transformed coarse-scale mobilities has to be added. This back transformation follows the rules discussed section 3.2, which are described in more detail in [27,30]. Here the back transformation is performed for the coarse-scale mobilities based on the numerically computed coarse-scale saturations. A Newton–Raphson method [24] has been used to solve equation (24). We repeat that the back transformation aims in finding a *homogeneous* fine-scale mobility in the upscaling cell, such that its transformed homogenized value is the same as the transformed homogenized value obtained from the original *heterogeneous* fine-scale mobility distribution. This way the principle of ‘conservation of homogeneity’ is fulfilled.

The results obtained for a number of computed coarse-scale saturations are given in table 3. As before, only values obtained with CN-FEM are reported. Both the no-capillary gradient case as well as the saturation-dependent capillary pressure case has been considered.

The results obtained with the two methods are summarized in figures 13–15. As a starting value the coarse-scale mobility value computed with CN-FEM was used in all runs.

As expected, the difference of mobility components in the z direction taken in the transformed and the original coordinate systems is almost negligible.

Because of the nonlinearity, the evaluation of the coarse-scale mobilities in the near-well region is much more computer time consuming than solving the problem in a rectangular domain. However, this additional cost is worth its price, since in this way we have not only satisfied the principle of ‘conservation of homogeneity’, but we have at the same time satisfied our requirement that, in the near-well region, the upscaled mobilities relate the *pressure difference* between well and outer boundary of the homogenization

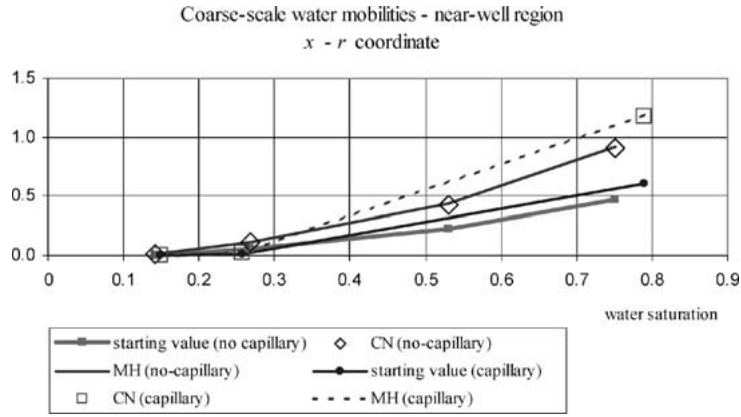


Figure 13. Back transform of the transformed coarse-scale mobility in r direction.

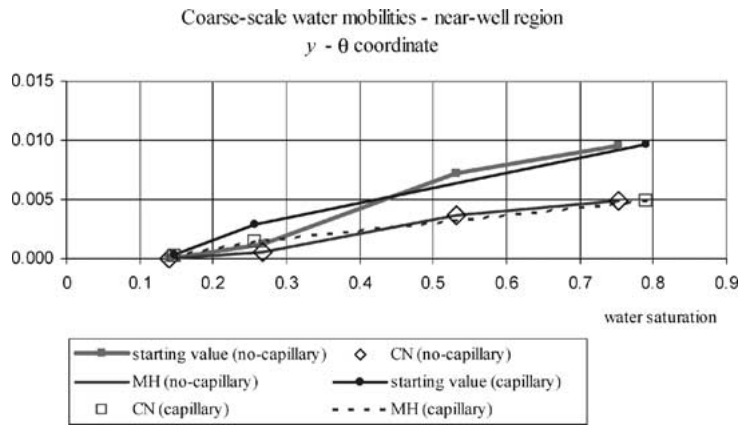


Figure 14. Back transform of the transformed coarse-scale mobility in θ direction.

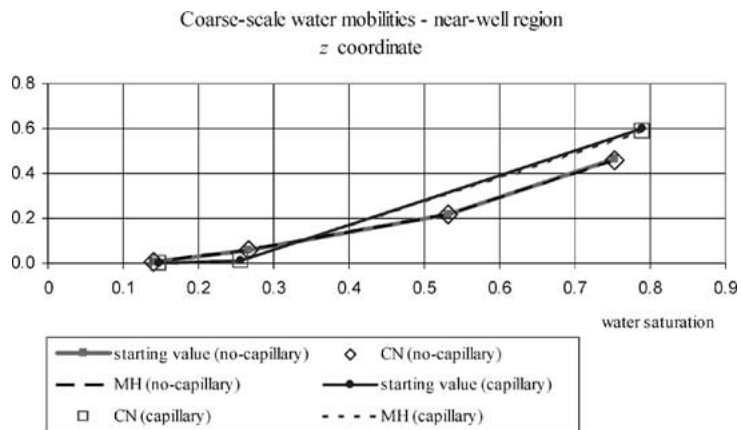


Figure 15. Back transform of the transformed coarse-scale mobility in z direction.

cell to the discharge rate of the well. This latter feature, which is important in many engineering applications, cannot be satisfied without solving equation (24).

5. Summary and conclusions

This paper deals with the numerical homogenization of the capillary pressure and the water and oil mobility in two-phase porous media. We discussed process-independent homogenization. This means that the resulting coarse-scale capillary pressure and the coarse-scale mobilities are functions of the coarse-scale saturation. These functions are independent from the scenario that is actually simulated by reservoir model in which these coarse-scale functions are used. We have given mathematical arguments supported by numerical examples showing that classical homogenization theory can be extended to nonlinear problems, also in near-well regions.

Our approach has been based on the principle of *preservation of form*, which states that the mathematical form of the fine-scale equations should be preserved *as much as possible* on the coarse scale. For the cases considered in this paper, this principle yields exactly the same results as the classical BLP theory for homogenization. This means that the mathematical convergence proofs of the BLP theory remain valid. In addition, the principle of preservation of form leads to practical extensions, while keeping the physical insight underlying homogenization transparent. In this context it is worth mentioning explicitly that application of this principle leads to a relation between pressure difference and flux. This is especially important in near-well regions, where engineering emphasis is on the pressure *difference* between well and reservoir, rather than on the averaged pressure gradient, as would be obtained using classical homogenization theory indiscriminately.

The resulting equations are elliptic partial differential equations of the Laplace type that cannot be solved analytically, except for a few special cases. Here the equations have been solved numerically by two complementary finite element methods:

- (i) the conformal-nodal finite element based on the ‘div-side equation’, and
- (ii) the mixed-hybrid finite element method based on the ‘curl-side equation’.

Although the div-side and curl side equation span the same solution space, the finite element approximations based on it are not equivalent. The div-side approximation yields upper bounds for the eigenvalues of the mobility tensor of each phase, while the curl-side approximation yields lower bounds. Using these two methods we are able to assess a posteriori bilateral error bounds, which serve as a check for the numerical quality of the results.

Acknowledgements

We gratefully acknowledge Alain Bossavit (Électricité de France) for his inspiring ideas. The support of the Banach Centre of Excellence (Warsaw) is gratefully acknowledged.

References

- [1] B. Amaziane and A. Bourgeat, Effective behavior of two-phase flow in heterogeneous reservoirs, numerical simulation in hydrocarbon recovery, in: *IMA Mathematics and its Applications*, Vol. 11, ed. M.F. Wheeler (Springer, Berlin, 1988) pp. 1–22.
- [2] B. Amaziane, A. Bourgeat and J. Koebbe, Numerical simulation and homogenization of two-phase flow in heterogeneous porous media, *Transport Porous Media* 9 (1991) 519–547.
- [3] J.W. Barker and P. Dupouy, An analysis of dynamic pseudo-relative permeability methods for oil-water flows, *Petroleum Geosci.* 5(4) (1999) 385–394.
- [4] J. Bear, *Dynamics of Fluids in Porous Media* (Dover, New York, 1988).
- [5] A. Bensoussan, L.-L. Lions and G. Papanicolaou, *Asymptotic Analysis for Periodic Structures* (North-Holland, Amsterdam, 1978).
- [6] A. Bossavit, *Computational Electromagnetism* (Academic Press, San Diego, 1998).
- [7] C.M. Case, *Physical Principles of Flow in Unsaturated Porous Media* (Oxford Univ. Press, New York, 1994).
- [8] L.J. Durlofsky, Use of higher moments for the description of upscaled process independent relative permeabilities, *SPE J.* 2 (1997) 474–84.
- [9] L.J. Durlofsky, An approximate model for well productivity in heterogeneous porous media, *Math. Geology* 32(4) (2000) 421–438.
- [10] L.J. Durlofsky, R.A. Behrens, R.C. Jones and A. Bernath, Scale up of heterogeneous three-dimensional reservoir descriptions, *SPE J.* (September 1996) 313–326.
- [11] L.J. Durlofsky, R.C. Jones and W.J. Milliken, A nonuniform coarsening approach for the scale-up of displacement processes in heterogeneous porous media, *Adv. in Water Resources* 20 (1997) 335–347.
- [12] L.J. Durlofsky, W.J. Milliken and A. Bernath, Scaleup in the near-well region, *SPE J.* 5(1) (2000) 110–117.
- [13] W.G. Gray, A. Leijnse, R.L. Kolar and C.A. Blain, *Mathematical Tools for Changing Spatial Scales in the Analysis of Physical Systems* (Lewis/CRC Press, Boca Raton, FL, 1993).
- [14] E.F. Kaasschieter and A.J.M. Huijben, Mixed-hybrid finite elements and streamline computations for the potential flow problem, *Numer. Methods Partial Differential Equations* 8 (1992) 221–226.
- [15] P.R. King, The use of renormalization for calculating effective permeability, *Transport Porous Media* 4 (1987) 37–58.
- [16] O. Mascarenhas and L.J. Durlofsky, Coarse scale simulation of horizontal wells in heterogeneous reservoirs, *J. Petroleum Sci. Engrg.* 25 (2000) 135–147.
- [17] P.M. Morse and H. Feshbach, *Methods of Theoretical Physics* (McGraw-Hill, New York, 1953).
- [18] M. Panfilov, *Macroscale Models of Flow through Heterogeneous Porous Media* (Kluwer, Dordrecht, 2000).
- [19] D.W. Peaceman, *Fundamentals of Numerical Reservoir Simulation* (Elsevier Science, Amsterdam, 1977).
- [20] D.W. Peaceman, Interpretation of well-block pressures in numerical reservoir simulation, *SPE J.* (June 1978) 183–194.
- [21] D.W. Peaceman, Interpretation of well-block pressures in numerical reservoir simulation with non-square grid blocks and anisotropic permeability, *SPE J.* (June 1983) 531–543.
- [22] G.E. Pickup, P.S. Ringrose and A. Sharif, Steady-state upscaling: From Lamina–Sclae to full-field model, *SPE J.* 5 (June 2000) 208–217.
- [23] G.E. Pickup and K.D. Stephen, An assessment of steady-state scale-up for small-scale geological models, *Petroleum Geosci.* 6 (2000) 203–210.
- [24] W.H. Press, S.A. Teukolsky, W.T. Vetterling and B.P. Flannery, *Numerical Recipes in FORTRAN: The Art of Scientific Computing* (Cambridge Univ. Press, New York, 1986).
- [25] R.F. Ribeiro and R.K. Romeu, Computing the effective permeability by finite differences, finite elements, and mixed-hybrid finite elements, *SPE* 39068 (1997).

- [26] X. Sánchez-Vila, C.L. Axness and J. Carrera, Upscaling transmissivity under radially convergent flow in heterogeneous media, *Water Resources Res.* 35(3) (1999) 613–621.
- [27] A. Trykozko, W. Zijl and A. Bossavit, Nodal and mixed finite elements for the numerical homogenization of 3D permeability, *Comput. Geosci.* 5 (2001) 61–84.
- [28] W. Zijl and M. Nawalany, *Natural Groundwater Flow* (Lewis/CRC Press, Boca Raton, FL, 1993).
- [29] W. Zijl and A. Trykozko, Numerical homogenization of the absolute permeability using the conformal-nodal and the mixed-hybrid finite element method, *Transport Porous Media* 44(1) (2001) 33–62.
- [30] W. Zijl and A. Trykozko, Numerical homogenization of the absolute permeability tensor around wells, *SPE J.* (2001) 399–408.